KBS TEKNISK RAPPORT

48

# The mechanical properties of the rocks in Stripa, Kråkemåla, Finnsjön, and Blekinge

Graham Swan

Högskolan i Luleå 1977-09-14

KÄRN - BRÄNSLE - SÄKERHET

POSTADRESS: Kärnbränslesäkerhet, Fack. 102 40 Stockholm. Telefon 08-67 95 40

# THE MECHANICAL PROPERTIES OF THE ROCKS IN STRIPA, KRÅKEMÅLA, FINNSJÖN AND BLEKINGE

Graham Swan
Högskolan i Luleå 1977-09-14

Denna rapport utgör redovisning av ett arbete som utförts på uppdrag av KBS. Slutsatser och värderingar i rapporten är författarens och behöver inte nödvändigtvis sammanfalla med uppdragsgivarens.

I slutet av rapporten har bifogats en förteckning över av KBS hittills publicerade tekniska rapporter i denna serie.

1977-09-14

# THE MECHANICAL PROPERTIES OF STRIPA GRANITE
KBS OBJECT PLAN 29:03

MATERIALEGENSKAPER HOS BERG

Graham Swan
Avd för bergmekanik
Högskolan i Luleå
Luleå

CONTENTS Side

# 1. SUMMARY

The mechanical properties of Stripa Granite are presented as determined from small (laboratory size), oven-dried specimens. The properties determined include Young´s modulus, Poisson´s ratio, unaxial compressive fracture stress and the expansion coefficient, all as a function of temperature.

In addition the Brazilian tensile fracture stress, residual shear strength as a function of a normal stress and the rock´s anisotropy ratios are presented. Finally ultrasonic determinations at 1 MHz of the rock´s dilatational wave velocity are given and the deduced Young´s modulus is compared with the static value for room temperature.

## 2. INTRODUCTION

For the determination of the mechanical properties of Stripa granite, samples were largely taken from the three boreholes Bh H1 (45 mm $\phi$), BH H2 (42 mm $\phi$) and Bh V1 (45/42 mm $\phi$). Addition samples were obtained from the 72 mm $\phi$ borehole Bh SI, "hand specimens" and from the orientated block B , see Fig 1. It was noticed that the granite type taken from these different sources is certainly of variable character. In an attempt to demonstrate this site variablility, selection of the samples for each test was made at random, rather than systematically taking adjacent samples from a common borehole. As a useful guide to this variability, in the results given below a comparision is made wherever possible with Bohus granite, a fairly uniform, well-known Swedish rock.

For the purposes of the numerical calculations later to be performed in Object 10:03, it was decided that the following parameters should be determined:

<u>3.1</u> Young´s modulus (E, GPa)
Poisson´s ratio ($\nu$)
Compressive fracture stress ($\sigma_c$, MPa)
Expansion coefficient ($\alpha$, $deg^{-1}C$)
} as a function of temperature $20 < t < 200^0C$

<u>3.2</u> Young´s modulus (E, GPa)
Compressive fracture stress ($\sigma_c$, MPa)
} as a function of confining pressure $0 < \sigma_3 < 30$ MPa

<u>3.3</u> Brazilian tensile fracture stress ($\sigma_T$, MPa)

<u>3.4</u> Residual shear stress ($\tau_r$, MPa) as a function of normal stress ($0 < \sigma_n < 11$ MPa)

<u>3.5</u> Anisotropy ratio´s for Young´s modulus (E, GPa) and compressive fracture stress ($\sigma_c$, MPa)

<u>3.6</u> Dilatational wave velocity ($C_1$, m/s) and deduced dynamic Young´s modulus ($E_{dyn}$, GPa)

Accompanying the results (3.1) through to (3.6) given below, is a brief description of the test method used.

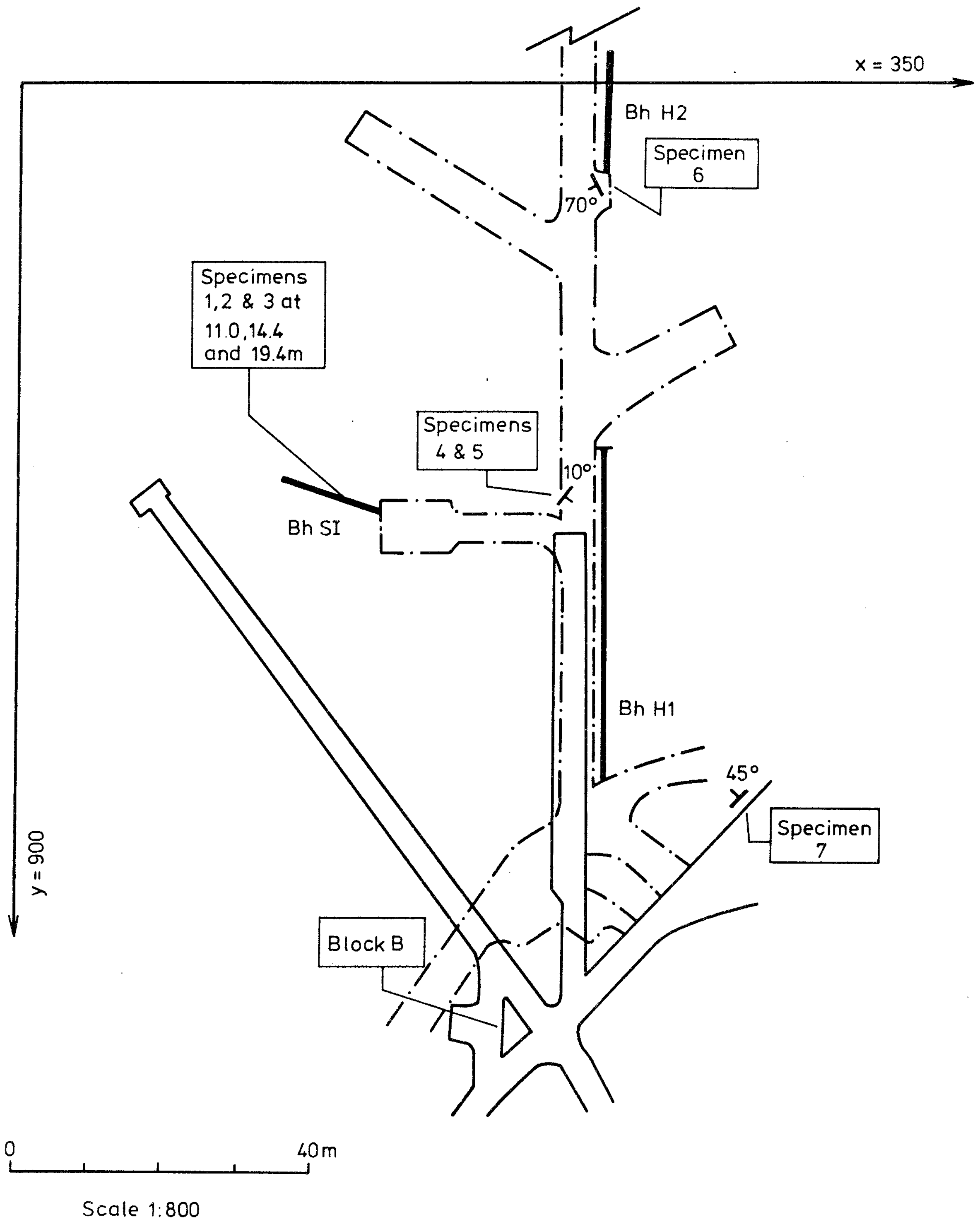


Fig. 1 Map showing locations from which test specimens have been taken, $P_{23}$ Stripa

# 3. RESULTS

## 3.1. Temperature dependency of Stripa Granite

The results for this group are derived from (i) a series of unaxial compression tests (obtaining E, $\nu$ and $\sigma_c$ as functions of temperature) and (ii) a theoretical calculation based on Simmon´s work [1] and experiments also developed by Simmon´s, which make use of a differential dilatometer [2] (obtaining the coefficient of cubical expansion $\alpha_v$ as a function of temperature).

### 3.1.1. Unaxial Compression tests

The specimens prepared for this test were 45 mm diameter cores cut to a length of 105 mm and oven-dried at $80^{O}C$ for 2 days. All strain measurements were made using strain gauges (type HBM 61 120 LY11, $20^{O} < T < 150^{O}C$ and type HBM 61 120 LG11, $T > 150^{O}C$) glued to the specimens. Each specimen was then lined with a thin plastic protection and heated for 2-3 hours in an oven to the predetermined equilibrium temperature. It was then placed into a heated oil bath and loaded to failure in a conventional unaxial compression test. At temperatures over $100^{O}C$ precautions were taken to eliminate gross heat losses from the oil bath via conduction and convection. Even so, because of the limitations of the method, it was only possible to maintain the high testing temperatures to within about ±5 % of the predetermined value.

From each test a plot of axial stress $\sigma_1$ against axial strain $\varepsilon_1$ and radial strain $\varepsilon_r$ was obtained, an example of which is shown in Fig 2. The values of E, $\nu$ and $\sigma_c$ derived from such a plot are given comprehensively in Table I. It should be noted that both E and $\nu$ are evaluated from secants drawn from the origin to intersect the curves at $\sigma_1 = 50\ \%\ \sigma_c$. A statistical summary of these results is given in Table II. Also appearing in Table II is the comparative data at room temperature for Bohus granite. The two rock types may also be compared in Plate 1 which shows the typical post-failure fracture surfaces resulting from the test. Graphical presentations of Table II are given in Figs 3 and 4.

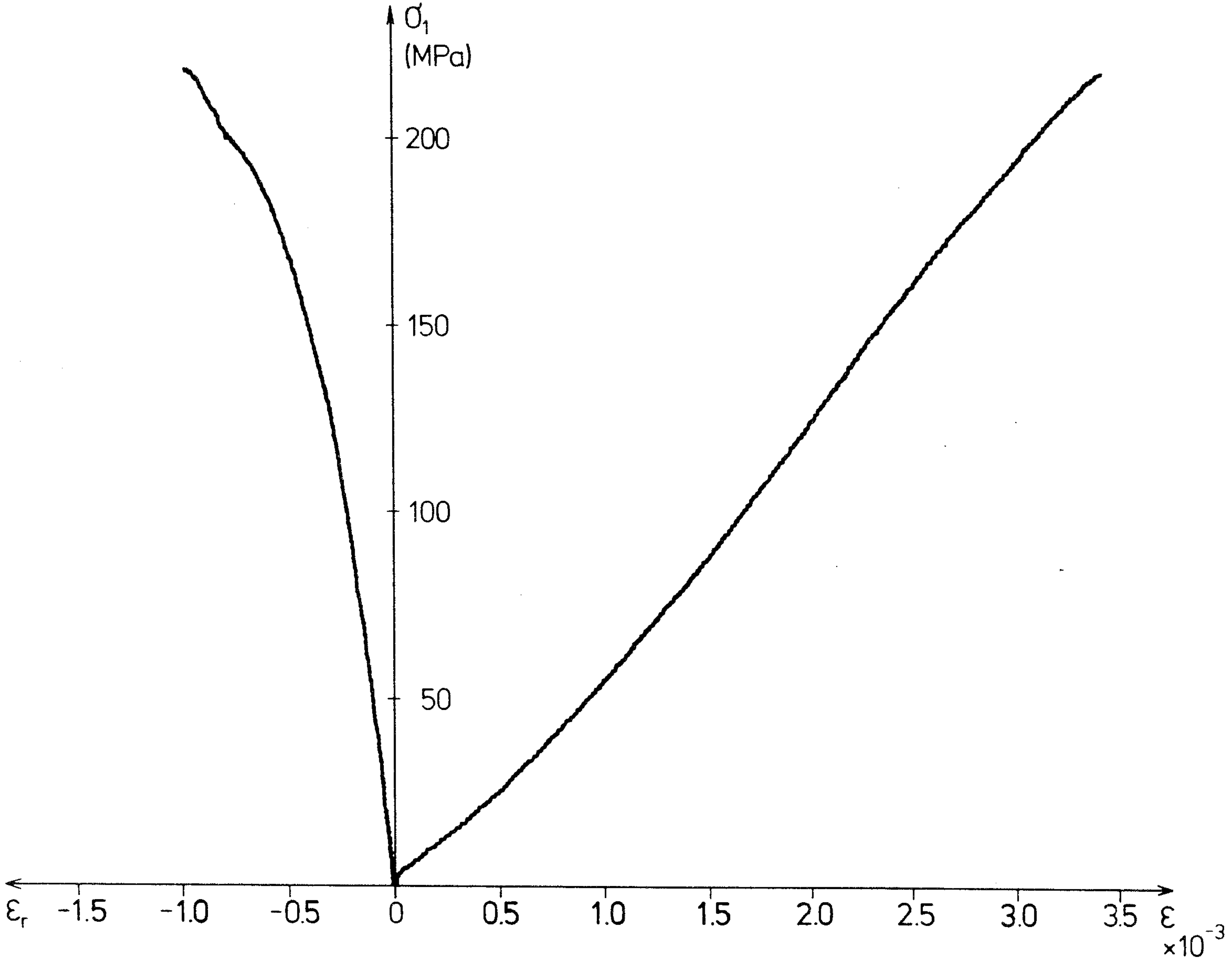


Fig. 2 TYPICAL STRESS vs STRAIN PLOT FROM UNIAXIAL TEST AT 150°C [Specimen E22]

Table I

Comprehensive results from unaxial Compression tests

| Oil bath temp. $^{o}C$ | Specimen number | Fracture stress $\sigma_c$ MPa | Young's Modulus E GPa | Poisson's ratio $\nu$ | Failure Description (see footnote) |
|---|---|---|---|---|---|
| 20 | V1 43.57 E1 | 192.0 | 72.4 | 0.27 | 1 |
| 20 | H1 33.30 E3 | 207.7 | 63.0 | - | 1 |
| 20 | V1 44.25 E5 | 229.9 | 67.4 | 0.23 | 2 |
| 20 | H1 30.10 E6 | 217.9 | 61.8 | 0.15 | 2 |
| 20 | V1 39.80 E7 | 180.9 | 78.4 | 0.23 | 1 |
| 20 | H1 29.25 E8 | 247.9 | 68.0 | 0.19 | 1 |
| 20 | H1 35.65 E9 | 222.0 | 64.0 | 0.20 | 1 |
| 20 | V1 44.70 E10 | 149.0 | 68.8 | 0.19 | 3 |
| 20 | H1 29.45 E11 | 245.6 | 67.8 | 0.20 | 1 |
| 20 | H1 28.60 E12 | 182.8 | 82.0 | 0.22 | 1 |
| | | | | | |
| 51-49 | V1 42.00 E31 | 177.8 | 70.2 | 0.18 | 2 |
| 50 | V1 52.36 E32 | 192.9 | 68.6 | 0.29 | 1 |
| 50 | H1 28.30 E33 | 200.6 | 67.4 | 0.23 | 1 |
| 50 | V1 44.35 E34 | 259.2 | 80.0 | 0.27 | 1 |
| 50 | V1 45.02 E35 | 228.7 | 67.6 | 0.19 | 1 |
| 50 | H1 29.35 E36 | 187.3 | 68.4 | 0.15 | 2 |
| 50 | H1 28.40 E37 | 231.4 | 73.4 | 0.20 | 1 |
| 50 | V1 44.60 E38 | 187.6 | 73.4 | 0.19 | 3 |

Note: 1 Complete failure

2 Partial failure: edge spall

3 Partial failure: weakness plane

Table I (contd)

| | | | | | |
|---|---|---|---|---|---|
| 105-73 | H1 24.00 E13 | 218.6 | 60.8 | 0.27 | 1 |
| 120-110 | H1 13.40 E14 | 249.0 | 57.8 | - | 1 |
| 100-92 | V1 39.31 E15 | 219.9 | 61.0 | 0.22 | 1 |
| 101-94 | V1 43.30 E16 | 213.1 | 62.6 | 0.22 | 2 |
| 101-96 | H1 14.45 E17 | 190.7 | 67.4 | 0.19 | 3 |
| 104-99 | H1 7.63 E18 | 228.7 | 61.6 | 0.18 | 1 |
| 102-97 | H1 16.35 E19 | 229.1 | 66.2 | 0.11 | 1 |
| | | | | | |
| 152-140 | H1 19.80 E20 | 208.2 | 60.6 | 0.17 | 2 |
| 155-151 | H1 16.45 E21 | 178.0 | 51.2 | 0.11 | 3 |
| 155-147 | H1 23.75 E22 | 217.6 | 60.0 | 0.13 | 1 |
| 155-148 | V1 39.21 E24 | 231.1 | 55.8 | 0.26 | 1 |
| 158-148 | H1 41.50 E25 | 212.0 | 53.6 | 0.15 | 1 |
| 157-150 | H1 31.80 E26 | 186.1 | 61.8 | 0.12 | 2 |
| | | | | | |
| 188-170 | H1 28.75 E29 | 194.9 | 47.6 | 0.20 | 2 |
| 197-175 | V1 44.12 E30 | 129.6 | 53.0 | - | 2 |
| 194-170 | V1 44.02 E39 | 143.1 | 49.6 | 0.09 | 2 |
| 197-180 | H1 29.62 E40 | 114.3 | 58.4 | 0.12 | 2 |
| 195-191 | V1 38.02 E41 | 155.9 | 44.6 | 0.14 | 2 |
| 195-180 | V1 38.12 E42 | 150.1 | 51.0 | 0.10 | 2 |

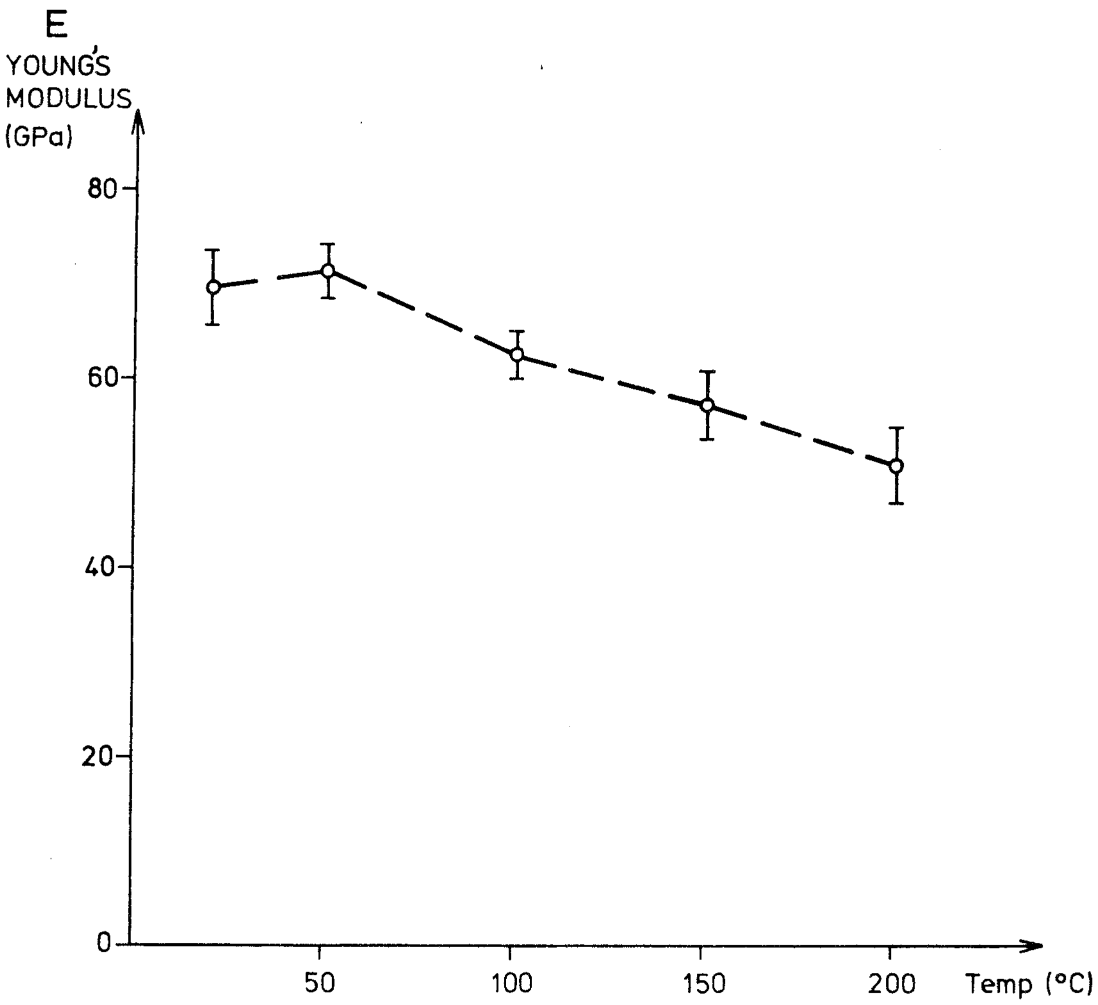


Fig. 3 YOUNG'S MODULUS vs TEMPERATURE showing 90% Confidence Limits

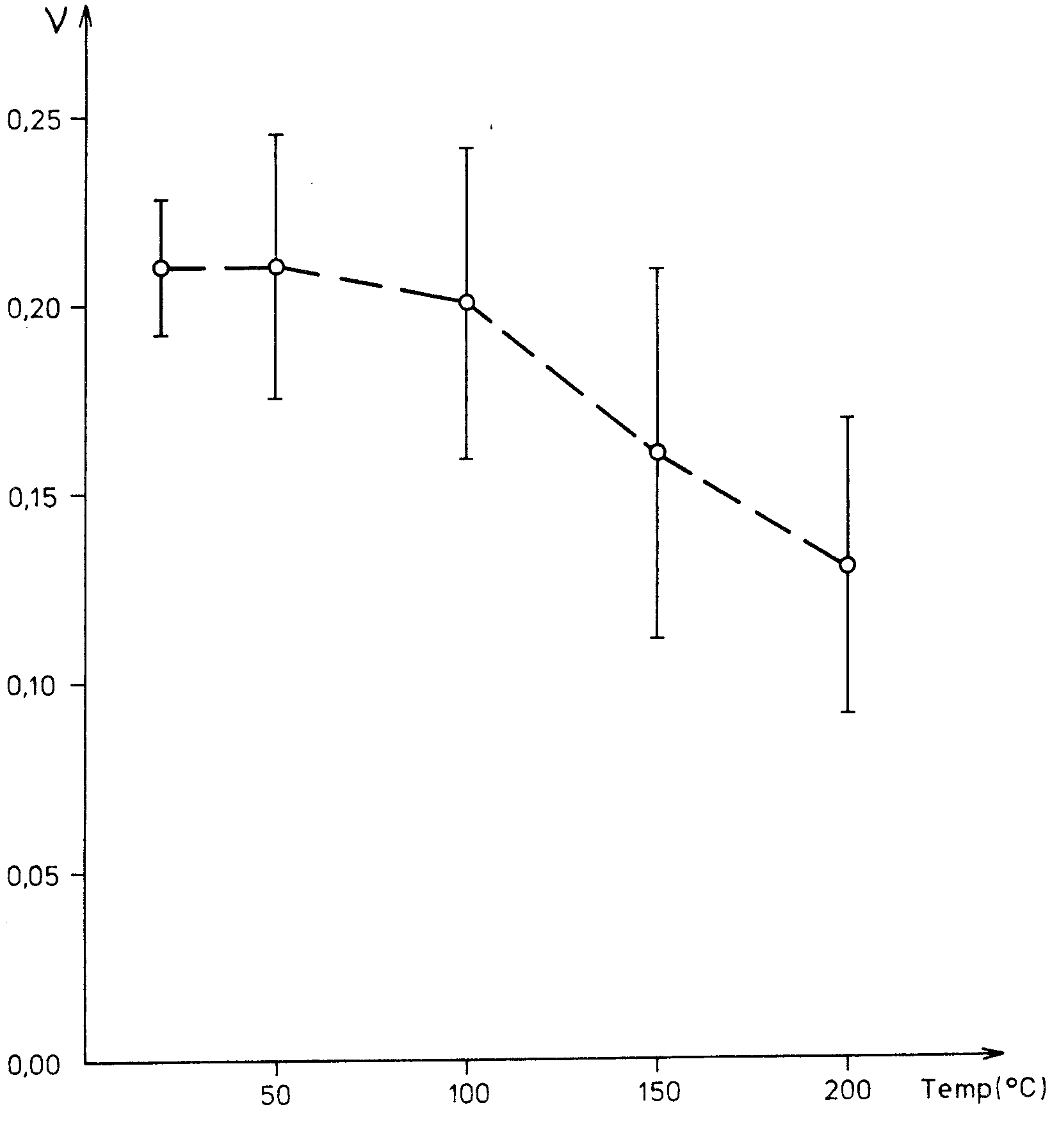


Fig. 4 POISSON RATIO vs TEMPERATURE
showing 90% Confidence Limits

Table II

Statistical Summary of Table I

| Sample Size | Mean Temp $^{o}C$ | Fracture Stress $\sigma_c$ MPa | | Young´s Modulus E GPa | | | Poisson´s Ratio $\nu$ | | |
|---|---|---|---|---|---|---|---|---|---|
| | | mean | standard dev. | mean | standard dev. | 90 % conf. lmts. | mean | standard dev. | 90 % conf. lmts. |
| 10 | 20 | 207.6 | 31.4 | 69.4 | 6.6 | 73.4<br>65.4 | 0.21 | 0.03 | 0.191<br>0.229 |
| 8 | 50 | 208.2 | 28.4 | 71.2 | 4.4 | 74.2<br>68.2 | 0.21 | 0.05 | 0.175<br>0.245 |
| 7 | 100 | 221.3 | 17.8 | 62.4 | 3.4 | 65.0<br>59.8 | 0.20 | 0.05 | 0.159<br>0.241 |
| 6 | 150 | 205.5 | 19.9 | 57.2 | 4.2 | 60.8<br>53.6 | 0.16 | 0.06 | 0.111<br>0.209 |
| 6 | 190 | 148.0 | 27.4 | 50.8 | 4.8 | 54.8<br>46.8 | 0.13 | 0.04 | 0.091<br>0.169 |
| Bohus Granite (Room temp) | | 157.0 | 43.0 | 53.3 | 2.6 | - | 0.20 | 0.01 | - |

### 3.2.1 Experimental determination of $\alpha_v$ as a function of temperature

The preliminary results* from $\alpha_v$ determinations on the Stripa granite are presented below in Table IV/V and in Fig 5/6. For the purpose of theoretically calculating $\alpha_v$ (see section 3.1.3) and for general reference, the modal composition of the light-red granite variety is given in Table III below.

Table III
Modal composition of Stripa granite.

| Mineral | Volume % |
|---|---|
| Quartz | 43.6 |
| Potash felspar | 12.0 |
| Plagiaclase felspar | 39.2 |
| Muscovite | 2.0 |
| Chlorite | 3.2 |
| Total | 100.0 |
| Number of points | 1 396 |

---

* supplied by Terra Tek and based on one sample only.

Table IV/V

| Temperature $^{o}C$ | Vol. expansion x $10^{-3}$ |
|---|---|
| 21 | 0.000 |
| 65 | 1.074 |
| 86 | 2.106 |
| 113 | 2.913 |
| 137 | 3.606 |
| 161 | 3.978 |
| 186 | 5.211 |
| 211 | 6.252 |
| 237 | 7.263 |

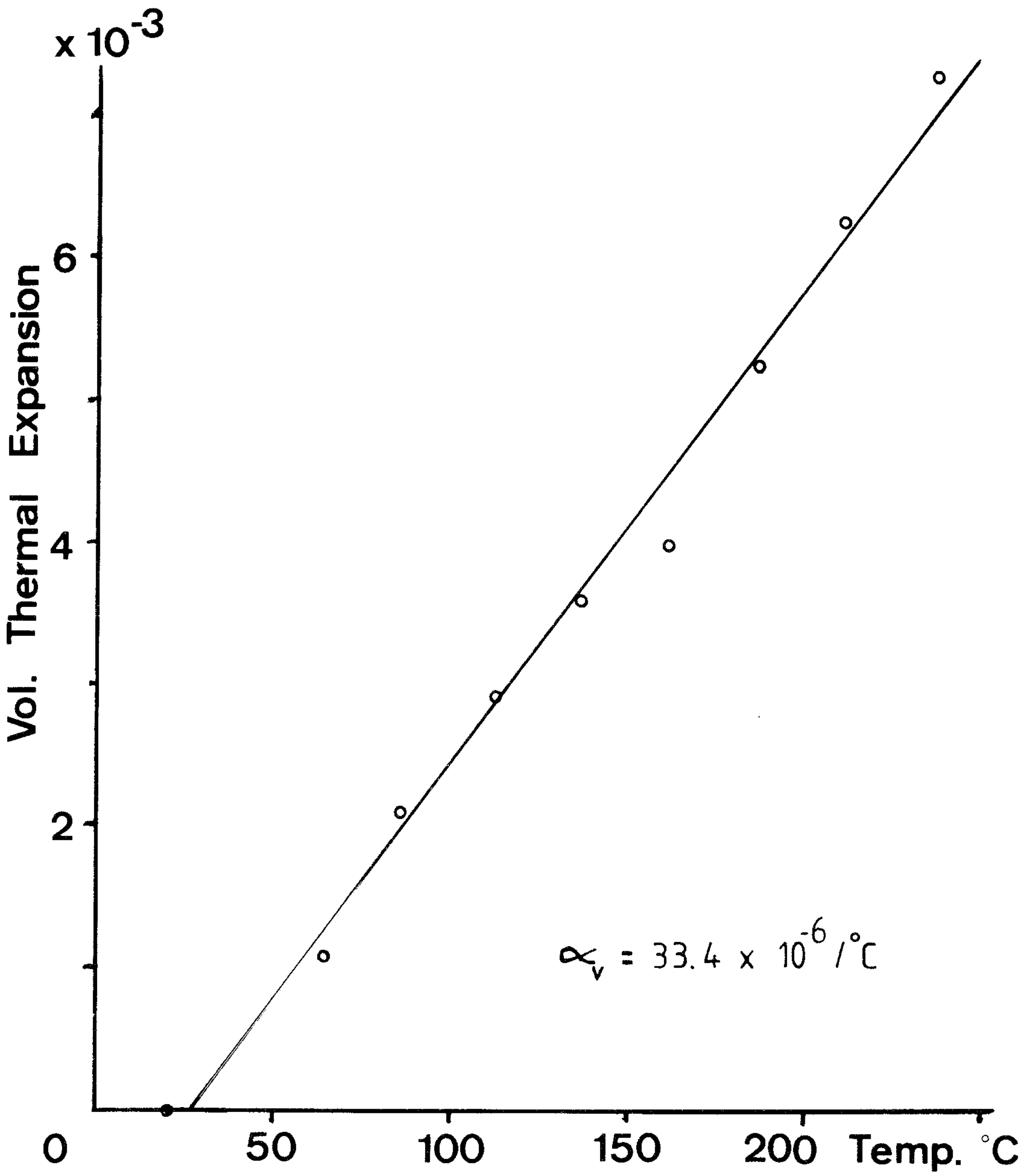


Fig 5/6. VOLUMETRIC THERMAL EXPANSION vs TEMPERATURE

### 3.1.3. Theoretical determination of $\alpha_v$ as a function of temperature

It has been shown by Cooper and Simmons [1] that $\alpha_v$ may be calculated theoretically for a number of different rock types and agreement with measured values, for the most part, is reasonably good. They obtained their theoretical $\alpha_v$ values using the composite expression:

$$\alpha_v = \frac{\Sigma \alpha_i E_i V_i}{\Sigma E_i V_i}$$

where $\alpha_i$ = coefficient of cubical expansion of $i^{th}$ phase
$E_i$ = Young´s modulus of $i^{th}$ phase
$V_i$ = volume fraction of $i^{th}$ phase

Tabel III gives the value of $V_i$ for the 5 phases occuring in Stripa granite. From the two available reference books [3] and [4] it is possible to extract data for $E_i$ and $\alpha_i$ for different minerals commonly found in granites (see Table VI).

Table VI
Data used for calculation of $\alpha_v$

| Mineral | $\alpha$ (25$^o$C) | $\alpha$ (400$^o$C) | E (GPa) |
|---|---|---|---|
| Quartz | 34 | 69 | 95.7 |
| K-felspar | 15 | 20 | 73.9 |
| Plagioclase | 13 | 17 | 88.1 |
| Muscovite | (20) | (25) | 78.8 |
| Biotite | (20) | (25) | 68.3 |
| Opaques | 29 | 45 | 230.5 |

These data have been used for the calculation of $\alpha_v$ both at $25^oC$ and at $400^oC$ for a number of granite types, including Stripa granite, Table VII. Included in this table are the comparative experimental and theoretical values given by Cooper and Simmons [1]. The reason for the discrepancy in the independantly calculated theoretical values remains, as yet, to be explained.

Table VII

Comparison between measured and calculated coefficients of thermal expansion

| Rock type | Specimen No | $\alpha_v(25^oC)x10^{-6}$ | | | $\alpha_v(400^oC)x10^{-6}$ | | |
|---|---|---|---|---|---|---|---|
| | | Experiment Ref.[1] | Theory Ref.[1] | Theory, Present work | Experiment Ref.[1] | Theory Ref.[1] | Theory, Present work |
| Stripa granite | - | - | 26.6 | 23.4 | - | 44.2 | 41.9 |
| Chelmsford granite | A757 | 21.5 | 25.3 | 21.2 | 73.3 | 37.5 | 36.3 |
| Westerly granite | 1134 | 24.8 | 22.6 | 19.6 | 67.0 | 32.9 | 32.1 |
| Wausau granite | 1343 | 19.9 | 27.2 | 23.4 | 71.5 | 41.0 | 41.8 |
| Graniteville granite | 1410 | 25.1 | 25.5 | 21.5 | 76.8 | 38.1 | 37.4 |
| Red River Quartzmon. | 1370 | 21.2 | 25.0 | 21.0 | 75.0 | 37.0 | 35.5 |

## 3.2. Triaxial Compression Tests

Specimens for the triaxial compression tests were taken from borehole H2, cut to lengths of 84 mm and oven dried at $80^{o}C$ for two days. Each specimen was then sealed in an impervious rubber jacket and placed in turn into a conventional triaxial cell. An electric oil pump with drain valves then maintained the equal minor principal stress level constant, while the axial load was increased in a 300 Ton machine to the specimen´s failure load. This load was noted for increasing values of confining pressure $0 < \sigma_3 = \sigma_2 < 30$ MPa.

The comprehensive data from these tests are given in Table VIII and the statistical summary in Table IX. A plot of axial stress $\sigma_1$ against axial strain $\varepsilon_1$ for different confining pressures as obtained from the tests is shown in Fig 7. The data of Table IX is also plotted, as seen in Fig 8. A typical barrell-shaped failed specimen is shown in Plate 2.

Table VIII

Comprehensive Results from Triaxial Compression Tests

| Confining Pressure $\sigma_3 = \sigma_2$ (MPa) | Specimen Number | Fracture Stress $\sigma_c$ (MPa) | Young's Modulus E (GPa) | Failure Description (see footnote) |
|---|---|---|---|---|
| 5 | H2 9.70 T22 | 302 | 75.4 | 1 |
| 5 | H2 51.35 T23 | 317 | 72.2 | 1 |
| 5 | H2 86.70 T24 | 319 | 75.6 | 1 |
| 5 | H2 84.25 T25 | 296 | 77.6 | 1 |
| 5 | H2 3.50 T26 | 266 | 76.2 | 2 |
| 10 | H2 85. 6 T7 | 352 | 76.8 | 1 |
| 10 | H2 5.50 T8 | 408 | 78.6 | 1 |
| 10 | H2 5.50 T10 | 384 | 77.4 | 1 |
| 10 | H2 42.15 T11 | 344 | 76.2 | 1 |
| 20 | H2 17.30 T12 | 476 | 83.0 | 1 |
| 20 | H2 5.90 T13 | 478 | 84.8 | 1 |
| 20 | H2 5.70 T14 | 462 | 83.8 | 1 |
| 20 | H2 73.20 T15 | 470 | 78.8 | 1 |
| 20 | H2 15.75 T16 | 464 | 80.6 | 1 |
| 30 | H2 9.90 T17 | 516 | 82.6 | 1 |
| 30 | H2 9.80 T18 | 480 | 82.8 | 2 |
| 30 | H2 15.65 T19 | 533 | 83.2 | 1 |
| 30 | H2 87.00 T20 | 520 | 83.2 | 1 |
| 30 | H2 15.90 T21 | 552 | 84.2 | 1 |

Note:
1 Complete failure
2 Failed on weakness plane

Table IX

Statistical Summary of Table VIII

| Confining Pressure (MPa) | Fracture stress $\sigma_c$ (MPa) | | Young´s Modulus E (GPa) | |
|---|---|---|---|---|
| | mean | standard deviation | mean | standard deviation |
| 5 | 308.5 | 9.8 | 75.4 | 1.78 |
| 10 | 372.0 | 25.6 | 77.2 | 0.88 |
| 20 | 470.0 | 6.3 | 82.2 | 2.20 |
| 30 | 530.3 | 14.0 | 83.2 | 0.56 |

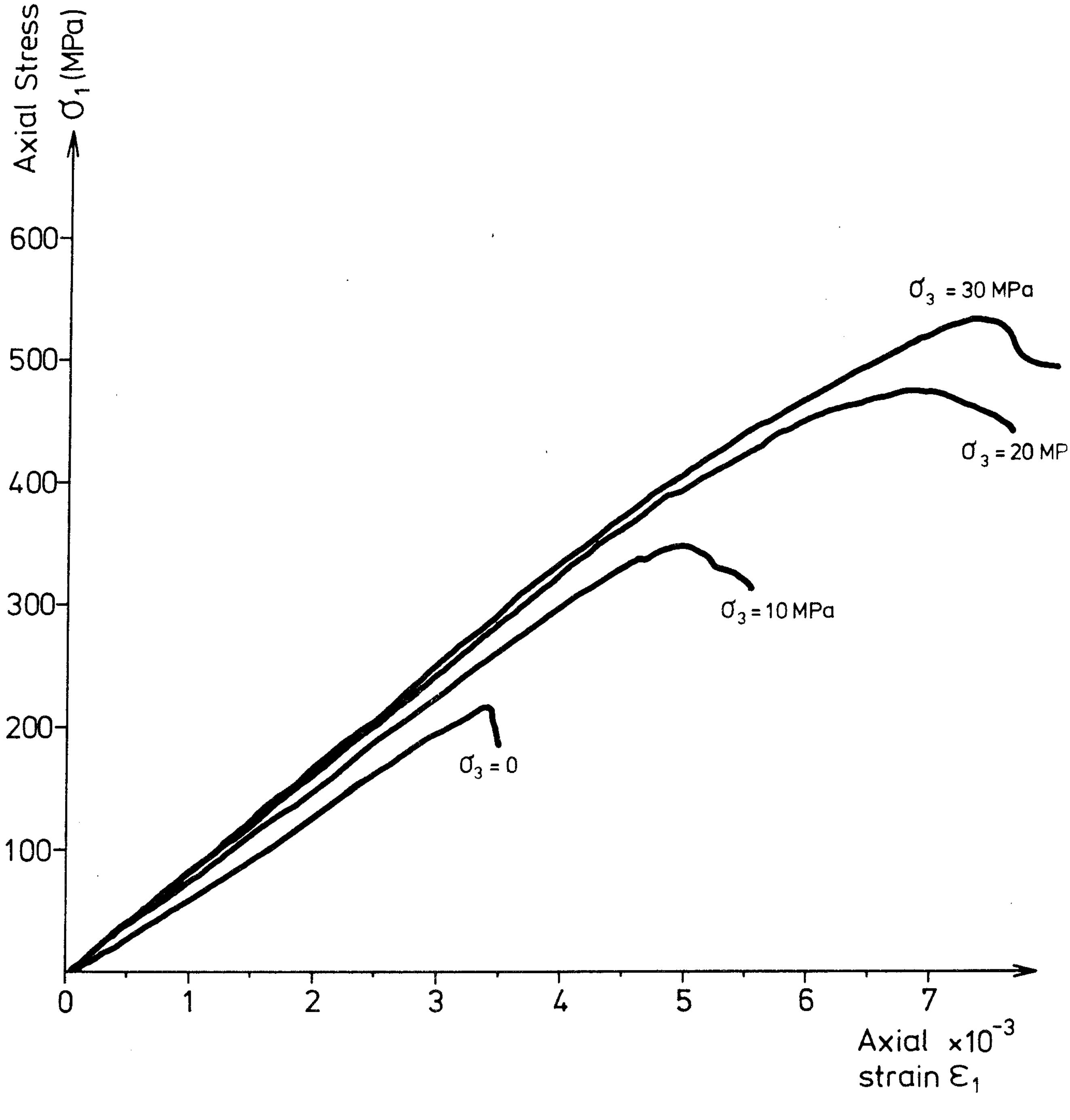


Fig.7 AXIAL STRESS vs STRAIN PLOTS FOR CONFINING PRESSURES $\sigma_2=\sigma_3$ OF 0,10,20 and 30 MPa.

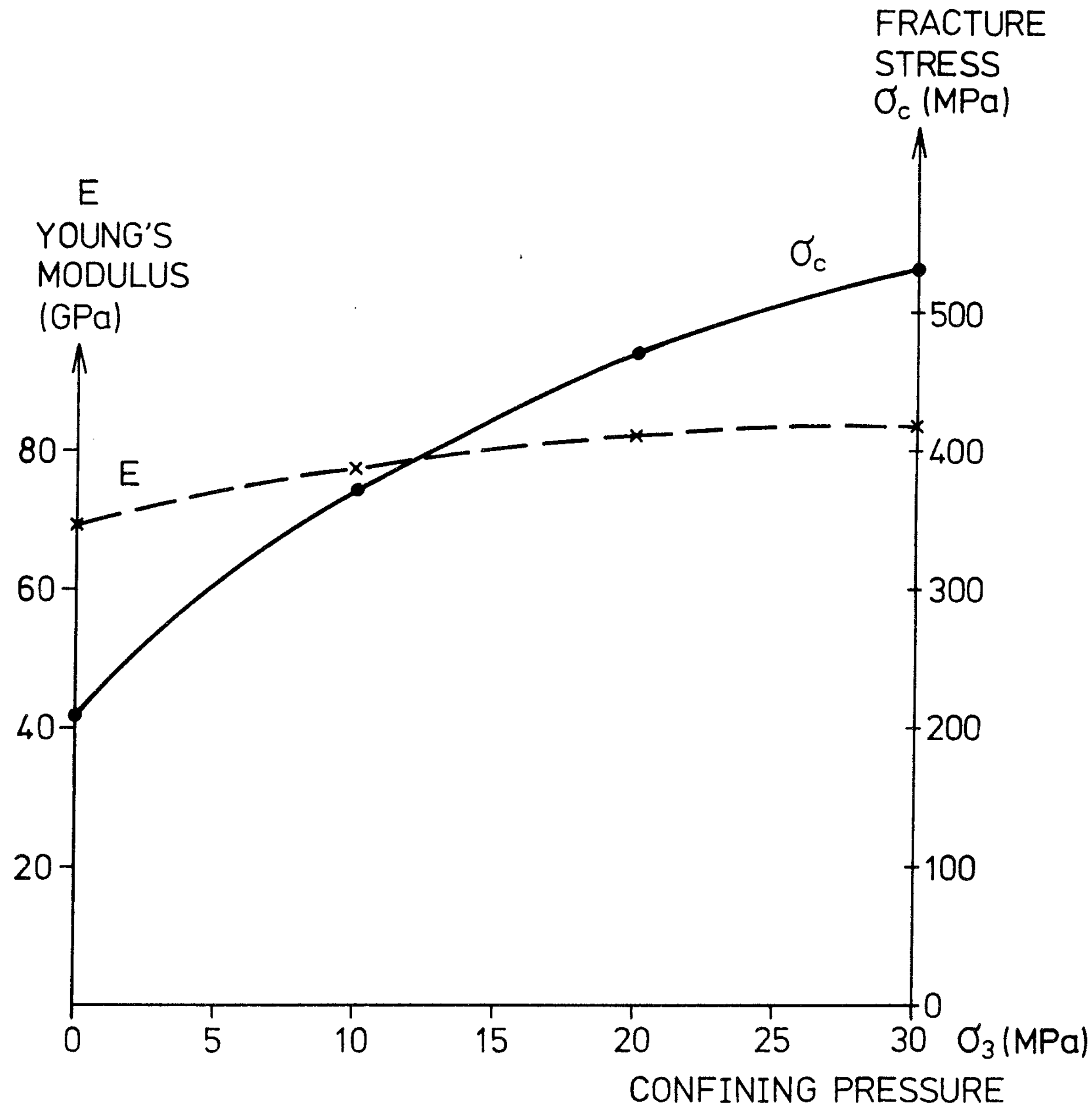


Fig.8 GRAPH SHOWING THE VARIATION OF YOUNG'S MODULUS AND FRACTURE STRESS $\sigma_c$ WITH CONFINING PRESSURE.

## 3.3. "Brazilian" tensile fracture tests

The specimens used in this test were taken from 72 mm diameter cores cut to lengths of 36 mm, and oven-dried for 2 days at $80^{o}C$. It only remained to compress each specimen under diametrically opposite loads and to note the failure load P. Ideally P should be the point failure load, but in practise local crushing occurs and so P is actually applied over a small angle $2\alpha$. The value of this angle was estimated to be $4.8^{o}$, from which the tensile failure stress was calculated using $\sigma_T = -2.45 \times 10^2 P$. The complete data from these tests is shown in Table X , as is also the statistical summary and the comparative values for Bohus granite.

Table X

Complete results from "Brazilian" tensile Fracture tests

| Specimen number | Failure Load P kN | Tensile fracture stress $\sigma_T$ MPa |
|---|---|---|
| B1 SI 4.41 | 61.2 | 14.99 |
| B2 SI 4.41 | 63.9 | 15.66 |
| B3 SI 1.55 | 67.5 | 16.54 |
| B4 SI 9.08 | 65.7 | 16.10 |
| B5 SI 9.08 | 56.7 | 13.89 |
| B6 SI 1.55 | 76.5 | 18.74 |
| B7 SI 9.60 | 60.3 | 14.77 |
| B8 SI 1.55 | 67.5 | 16.54 |
| B11 SI 9.08 | 51.3 | 12.57 |
| B15 SI 9.60 | 54.0 | 13.23 |
| B16 SI 6.53 | 54.0 | 13.23 |
| B17 SI 6.53 | 54.0 | 13.23 |

| | "Brazilian" fracture stress $\sigma_T$ | | |
|---|---|---|---|
| | mean MPa | standard deviation | 90 % Conf. limits |
| Stripa granite | 14.96 | 1.75 | 13.9<br>15.9 |
| Bohus granite | 10.50 | 0.63 | - |

## 3.4 Laboratory Shear Box tests

Specimens for this test were selected from 72 mm diameter cores and from hand specimens (see Fig 1 for locations) all having natural joint surfaces. Each specimen was first oven-dried and then encapsulated in a concrete mould (see Plate 3). The equipment used for the test was a standard Robertson's field shear box. A general description of each joint surface tested is given in Table XI. The dominating fill material in all cases was chlorite. A plot showing the dependency of residual shear strength ($\tau_r$) on joint normal pressure ($\sigma_n$, $0 < \sigma_n < 11$ MPa) is shown in Fig 9. It is apparent from this figure that the residual shear strength may be described by the bilinear relationships:

$$\sigma_r = \sigma_n \tan\phi_{r1}, \qquad 0 < \sigma_n < 3.4 \text{ MPa}$$

where $\phi_{r1} = 32.7^0$

and

$$\sigma_r = \sigma_n \tan\phi_{r2} + S_o, \qquad 3.4 < \sigma_n < 11 \text{ MPa}$$

where $\phi_{r2} = 24.8^0$ and $S_o = 0.71$ MPa

The upper limit of 11 MPa in the second equation is fixed by the strength of the encapsulating material (concrete) of the test, and by the joint area of the specimen. Predictions made outside the above stated limits should be treated cautiously.

Table XI

General description of joints tested

| Specimen number | Joint surface Area ($cm^2$) | Joint fill thickness (mm) | Surface structure (see footnote) |
|---|---|---|---|
| 1 | 44.60 | 1-3 | 1 |
| 2 | 44.50 | 0-1 | 3 |
| 3 | 40.80 | 0-1 | 2 |
| 4 | 46.35 | 1-3 | 1 |
| 5 | 31.10 | 1-3 | 2 |
| 6 | 39.20 | 0.5-1 | 2 |
| 7 | 35.60 | 1-2 | 2 |

Notes:
1. Dominantly plane
2. Plane with rough irregularities
3. Plane with marked roughness

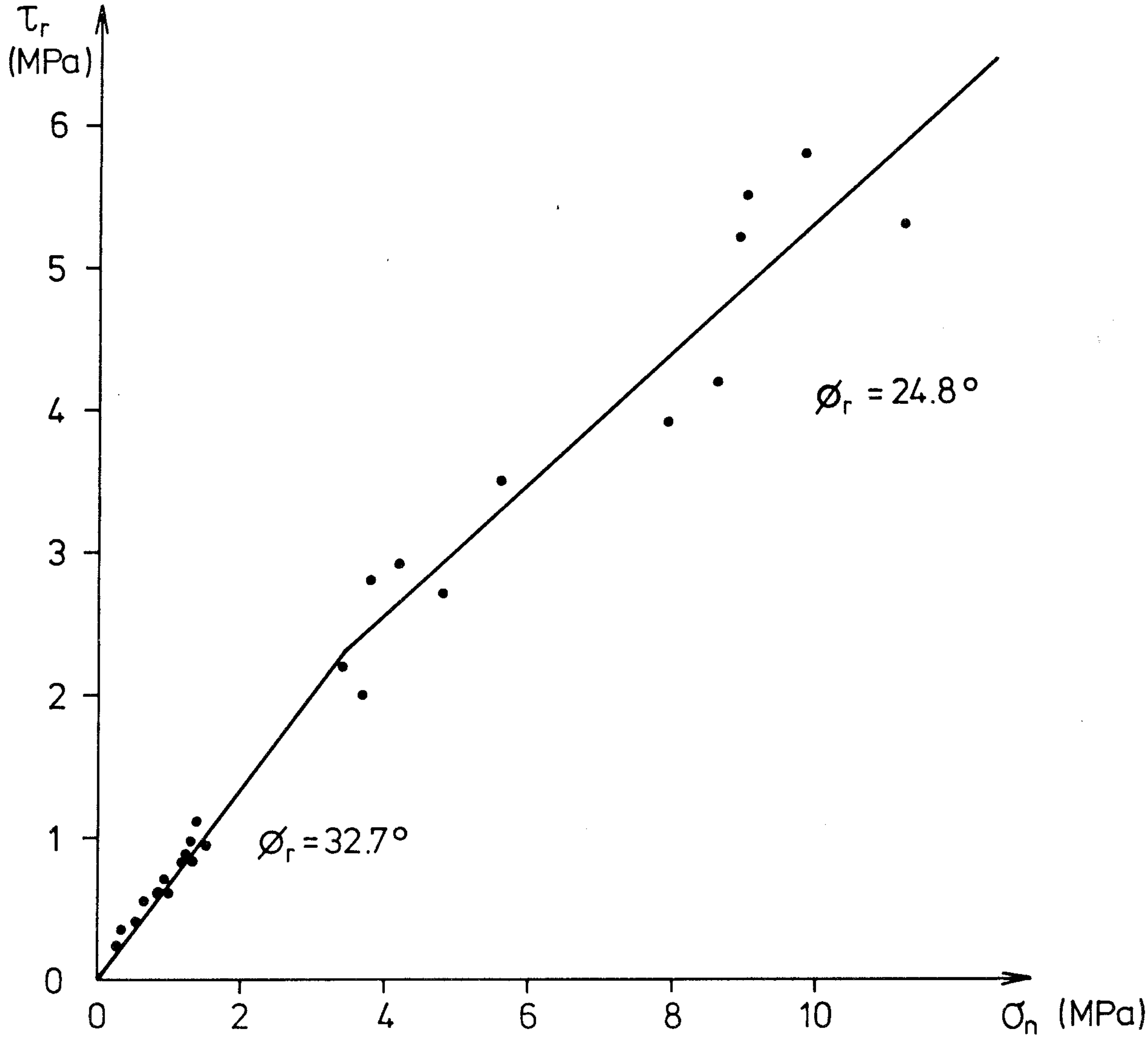


Fig. 9 Residual Shear Strength $\tau_r$ as a function of normal joint pressure $\sigma_n$

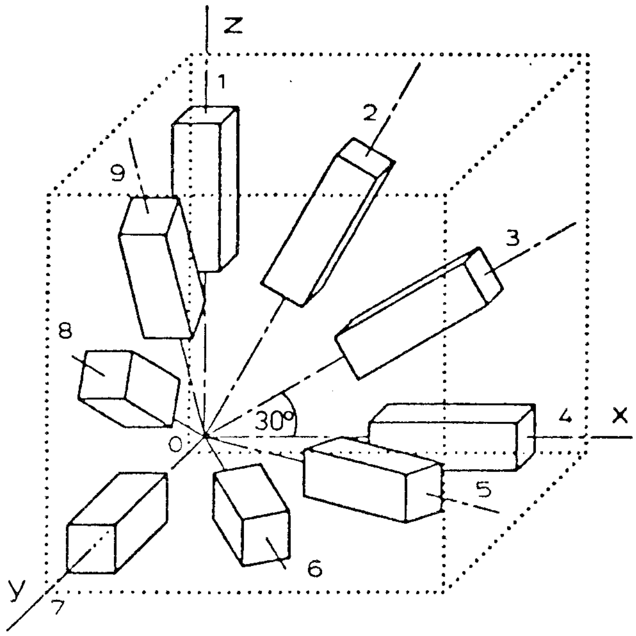


Fig. 10 SAMPLING CONFIGURATION FOR FULL-SCALE ANISOTROPY TEST.

provkropparna är cylindriska.

## 3.5. Anisotropy Tests

In order to measure the anisotropy in a material like granite it is necessary to take extensive samples from a coordinated block in the manner shown, Fig 10. For this purpose a block with known orientation was taken from the Stripa mine and from this block it was proposed to recover 5 core specimens 42 mm $\phi$ x 84 mm length from each angled holc. Unfortunately, owing to the jointed state of the block, core recovery was poor. It was therefore decided that instead of completing the full-scale anisotropy tests as planned, a small-scale test in one plane (x-z plane) would serve as an indication of anisotropy. The variables in which anisotropy should be observed were taken to be Young´s modulus, compressive fracture stress and dilatational wave velocity.

The complete results from these tests are given in Table XII. The sample size of 2 for each angle is not of course acceptable for a definative statement on anisotropic behaviour. However a trend is apparent in the sampled x-z plane both with regard to Young´s modulus and dilatational wave velocity.

Table XII

Small-scale anisotropy test results

| Specimen number | Density | $C_1$ Wave velocity | | E Young´s Modulus | | $\sigma_c$ |
|---|---|---|---|---|---|---|
| | | | mean | | mean | |
| | ($kg/m^3$) | (m/s) | s.d. | (GPa) | s.d. | (MPa) |
| B1.1 | 2616.9 | 5164.2 | 5180.3 | 66.8 | 64.9 | 227.4 |
| B1.2 | 2616.9 | 5196.3 | ±16.1 | 63.0 | ±2.0 | 81.2 |
| B2.1 | 2614.4 | 5268.8 | 5240.9 | 65.8 | 65.2 | 237.2 |
| B2.2 | 2609.8 | 5213.0 | ±27.9 | 64.6 | ±0.6 | 227.4 |
| B3.1 | 2613.8 | 5310.1 | 5311.1 | 64.4 | 65.5 | 207.6 |
| B3.2 | 2616.3 | 5312.1 | ±1.0 | 66.6 | ±1.2 | 233.9 |
| B4.1 | 2617.8 | 5353.5 | 5381.6 | 64.4 | 65.7 | 181.2 |
| B4.2 | 2619.7 | 5409.7 | ±28.1 | 67.0 | ±1.4 | 234.8 |

## 3.6. Dilatational Wave velocity measurements

Dilatational wave velocities ($C_1$) were measured in oven dried cylindrical specimens cut to lengths of 105 mm. Travel times were determined over this path length by an ultrasonic pulse technique at 1 MHz. The data obtained in this way together with the measured specimen densities is shown in Table XIII. Knowing the unconfined Young's modulus and Poisson's ratio (see Table III) it is possible to calculate a theoretical value for $C_1$. This value is also given in Table XIII where it is seen to be approximately 5 % higher than the observed value of 5213 m/s. Alternatively, knowing $C_1$ experimentally and assuming $\nu_{dynamic} = \nu_{static}$, a dynamic value for Young's modulus $E_{dyn}$ may be estimated to have a value ≃ 63.3 GPa. However, in order to obtain $E_{dyn}$ more precisely it is necessary to measure the distortional wave velocity, but this has not been done in the present work.

Table XIII

Density and Dilatational wave velocity data and results

| Specimen number | Density $\rho$ ($kg/m^3$) | Dilatational Wave velocity $C_1$ (m/s) |
|---|---|---|
| H2 6.60 | 2619 | 5123 |
| H2 10.02 | 2630 | 5117 |
| H2 10.13 | 2622 | 5132 |
| H2 14.87 | 2625 | 5266 |
| H2 30.57 | 2616 | 5230 |
| H2 31.04 | 2521 | 5261 |
| H2 31.15 | 2625 | 5255 |
| H2 64.19 | 2627 | 5187 |
| H2 77.23 | 2617 | 5296 |
| mean | 2622.5 | 5213.8 |
| standard deviation | 4.2 | 64.8 |
| Calculated dilatational wave velocity $C_1 = [E(1-\nu)/(1+\nu)(1-2\nu)\rho]^{1/2}$ | | 5457.9 |

## 4. DISCUSSION

The Stripa granite as taken from the site locations of Fig 1 is a relatively coarse-grained material which on the scale of laboratory testing strongly exhibits linearly elastic behaviour. In comparison with other granites both its Young´s modulus and its compressive fracture stress is high. This is likely to be accounted for by its high quartz content. The temperature dependancy of its elastic properties within the range $25 < T^{o}C < 200$ are similar to those of a granite reported elsewhere [5]. The large-scale properties of Stripa granite will to a great extent be determined by its strongly jointed (fractured) nature. This may be inferred with even greater certainty where chlorite-filled joints exist as a result of retrograde metamorphism.

## 5. ACKNOWLEDGEMENT

The assistance of Thomas Olofsson and Kenneth Mäki in the preparing and testing of rock specimens is gratefully acknowledged. Thanks is also due to Ove Alm for help and advice in the triaxial testing and to those at M.I.T., Dept of Earth and Planetary Sciences, who kindly supplied experimental data for the thermal expansion of the rock.

## 6. REFERENCES

[1] The effect of cracks on the thermal expansion of rocks, Cooper H. W. and Simmons G., Earth and Planetary Sc Letters, 1977 (in press)

[2] Thermal expansion behaviour of Igneous rocks, Richter D. and Simmons G., Int Jnl Rock Mech Min Sc, Vol 11, pp 403-411, 1974

[3] Thermal Expansion, Skinner B, J., in Handbook of Physical Constants, G.S.A. Memoir 97, p 75, 1966

[4] Single Crystal Elastic Constants and Calculated Aggregate Properties, Simmons G. and Wang H., M.I.T. press, Cambridge, 1971

[5] Thermal Guidelines for a Repository in Bedrock, Published Report of Parsons Brinckerhoff Quade & Douglas, Inc, New York, 1976

# 7. PLATES

Plate 1

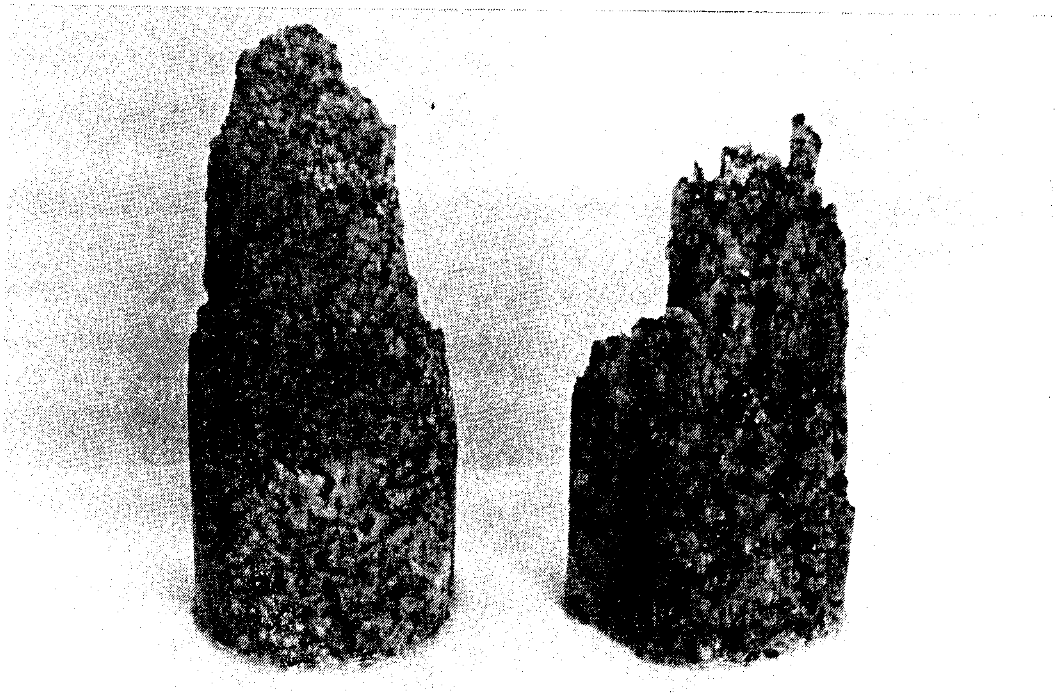

Appearance of failed specimens after unaxial compression test, Bohus granite left, Stripa granite right.

Plate 2 A

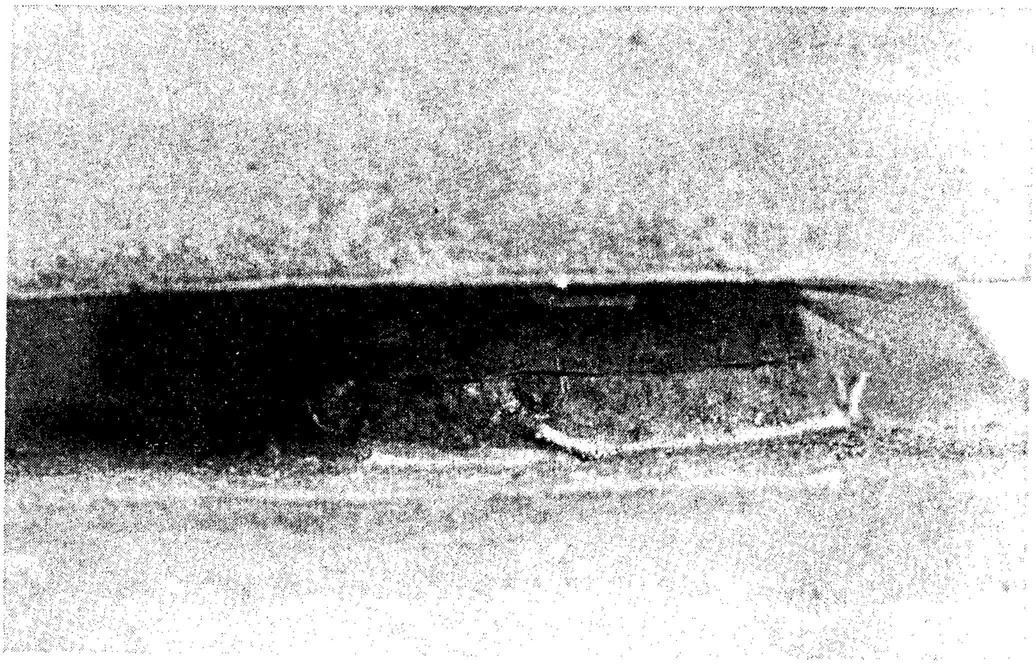

A jointed specimen shown encapsulated in concrete.

Plate 2 B

Appearance of a natural joint surface. The dark features are due to the presence of chlorite.

Plate 3

Appearance of failed specimen after triaxial compression test, $\sigma_3 = \sigma_2 = 20$ MPa. The rubber surround has been cut away after the test.

# THE MECHANICAL PROPERTIES OF THE KRÅKEMÅLA, FINNSJÖN AND BLEKINGE ROCKS.

KBS OBJECT PLAN 24:01

FÖRARBETEN FÖR PLATSVAL,

BERGMEKANISK PARAMETERBESTÄMNING

Graham Swan
Avd för bergmekanik
Högskolan i Luleå
Luleå

CONTENTS

# 1. SUMMARY

The mechanical properties of Kråkemåla granite, Finnsjön granodiorite and Blekinge gneiss are presented as determined from small (laboratory size), oven-dried specimens. The properties determined include Young´s Modulus, Poisson´s ratio, uniaxial compressive fracture stress and the Brazilian tensile fracture stress, all at room temperature.

## 2. INTRODUCTION

For the determination of the mechanical properties of each rock type, samples were taken at three different sites in each borehole viz. shallow depth (0-100), medium (200-300 m) and deep (400-500 m). The core size available were either of diameter 42 mm or 45 mm, which in the case of uniaxial compression testing were cut to sample lengths such that (L/D) was 2.5.

# 3. RESULTS

## 3.1 Kråkemåla Granite

For the two boreholes (KR 1 and KR 2) from the Kråkemåla site, uniaxial compression test data is presented in Table Ia, while Fig. 1 shows a typical plot of axial stress against axial strain $\varepsilon_1$ and radial strain $\varepsilon_r$. A statistical summary of this data appears in Table Ib. The typical appearance of a failed specimen is shown in Plate 1.

The "Brazilian" tensile fracture stress data for the rock was obtained by compressing specimens (42 mm $\phi$) under diametrically opposite loads and noting the failure load P. The complete data for these tests are given in Table IIa together with a statistical summary in Table IIb. The appearance of a broken specimen is shown in Plate 2.

## 3.2 Finnsjön Granodiorite

For the single borehole (FI 1) from the Finnsjön site, uniaxial compression test data is presented in Table IIIa, while Fig. 2 shows a typical plot of axial stress against axial strain $\varepsilon_1$. A statistical summary of this data appears in Table IIIb. The appearance of a failed specimen of this rock type is shown in Plate 3.

The complete data for the "Brazilian" tensile tests on the rock are given in Table IVa together with a statistical summary in Table IVb. The appearance of a broken specimen is shown in Plate 4.

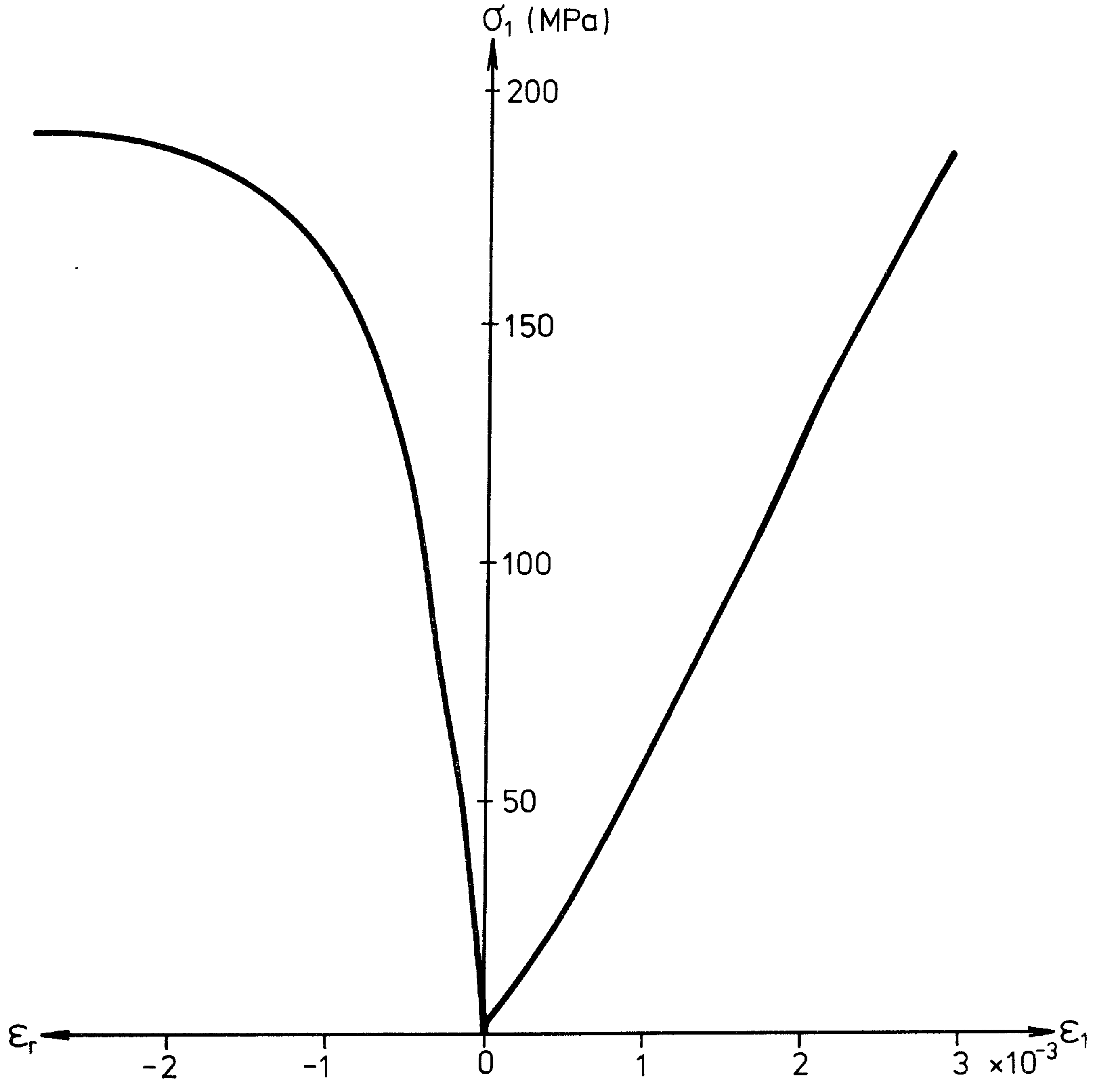


**Fig 1** TYPICAL STRESS-STRAIN PLOT FROM UNIAXIAL COMPRESSION TEST: KRÅKEMÅLA GRANITE.

PLATE 1

Appearance of failed specimen after uniaxial compression test: Kråkemåla granite.

PLATE 2

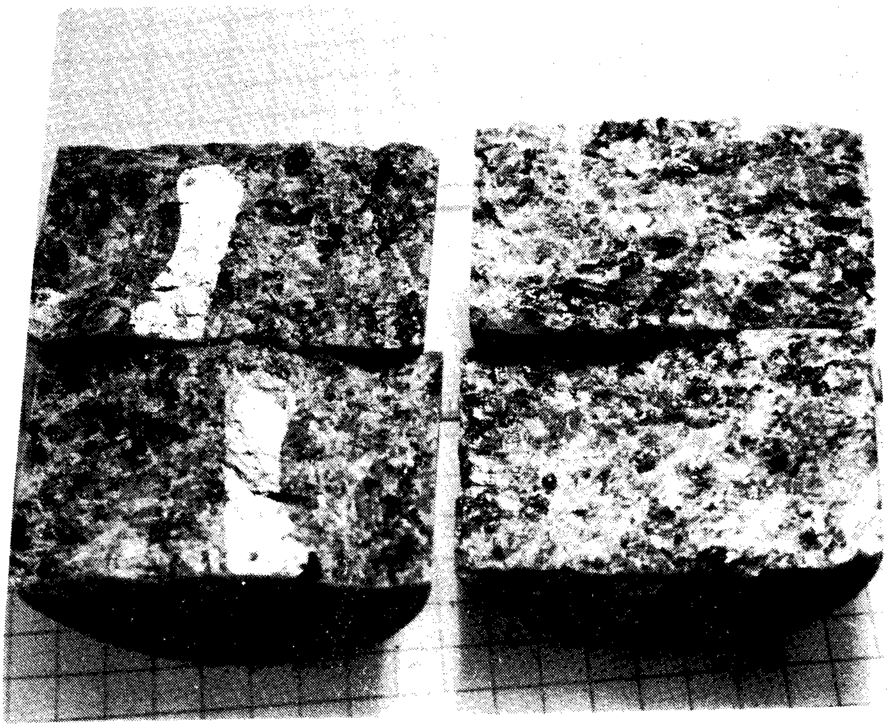

Appearance of failed specimens after Brazilian test: Kråkemåla granite. Note the coarseness of the crystalline structure.

Table Ia

Comprehensive data: uniaxial compression tests

| Specimen number | Fracture stress $\sigma_c$ (MPa) | Young´s Modulus E* (GPa) | Poisson´s ratio $\nu$ | Failure Description (see footnote) |
|---|---|---|---|---|
| KR 22.20 H1 | 225.1 | 63.9 | 0.23 | 2 |
| KR 23.85 H1 | 190.7 | 59.6 | 0.25 | 2 |
| KR 212.60 H1 | 188.0 | 61.0 | 0.23 | 2 |
| KR 213.30 H1 | 176.1 | 57.5 | 0.16 | 2 |
| KR 464.05 H1 | 177.4 | 56.7 | 0.17 | 2 |
| KR 465.20 H1 | 172.1 | 69.4 | 0.18 | 2 |
| | | | | |
| KR 18.50 H2 | 176.1 | 61.5 | 0.15 | 2 |
| KR 19.60 H2 | 143.0 | 51.6 | 0.22 | 2 |
| KR 305.30 H2 | 131.1 | 54.1 | - | 2 |
| KR 306.57 H2 | 152.3 | 68.6 | 0.28 | 2 |
| KR 563.20 H2 | 135.0 | 48.2 | 0.16 | 2 |
| KR 564.40 H2 | 178.7 | 58.4 | 0.24 | 2 |

Table Ib

Statistical summary, KRÄKEMÅLA Holes 1 and 2

| KR - H1 | $\sigma_c$ (MPa) | E* (GPa) | $\nu$ |
|---|---|---|---|
| mean | 188.2 | 61.4 | 0.20 |
| standard deviation | 17.8 | 4.3 | 0.03 |
| | | | |
| KR - H2 | $\sigma_c$ (MPa) | E* (GPa) | $\nu$ |
| mean | 152.7 | 57.1 | 0.21 |
| standard deviation | 18.7 | 6.7 | 0.05 |

*Secant modulus at 50 % failure load

Note: 1. vertical splitting
2. failure on on inclined plane (s)

Table IIa

Comprehensive data: "Brazilian" tests

| Specimen number | Failure Load P (kN) | Tensile fracture stress $\sigma_T$ (MPa) |
|---|---|---|
| KR 22.1 H1 | 16.92 | 10.4 |
| KR 22.1 H1 | 14.76 | 9.1 |
| KR 212.1 H1 | 14.58 | 9.0 |
| KR 212.1 H1 | 14.22 | 8.7 |
| KR 464.6 H1 | 11.70 | 7.2 |
| KR 464.6 H1 | 14.76 | 9.1 |
| | | |
| KR 18.5 H2 | 15.84 | 9.7 |
| KR 18.5 H2 | 12.96 | 8.0 |
| KR 305.1 H2 | 8.28 | 5.1 |
| KR 305.1 H2 | 9.90 | 6.1 |
| KR 564.4 H2 | 9.90 | 6.1 |
| KR 564.4 H2 | 9.18 | 5.6 |

Table IIb

Statistical summary, KRÅKEMÅLA Holes 1 and 2

| "Brazilian" fracture stress $\sigma_T$ | | |
|---|---|---|
| Rock Type | mean (MPa) | standard deviation |
| KRÅKEMÅLA Bh 1 | 8.92 | 0.94 |
| KRÅKEMÅLA Bh 2 | 6.77 | 1.59 |

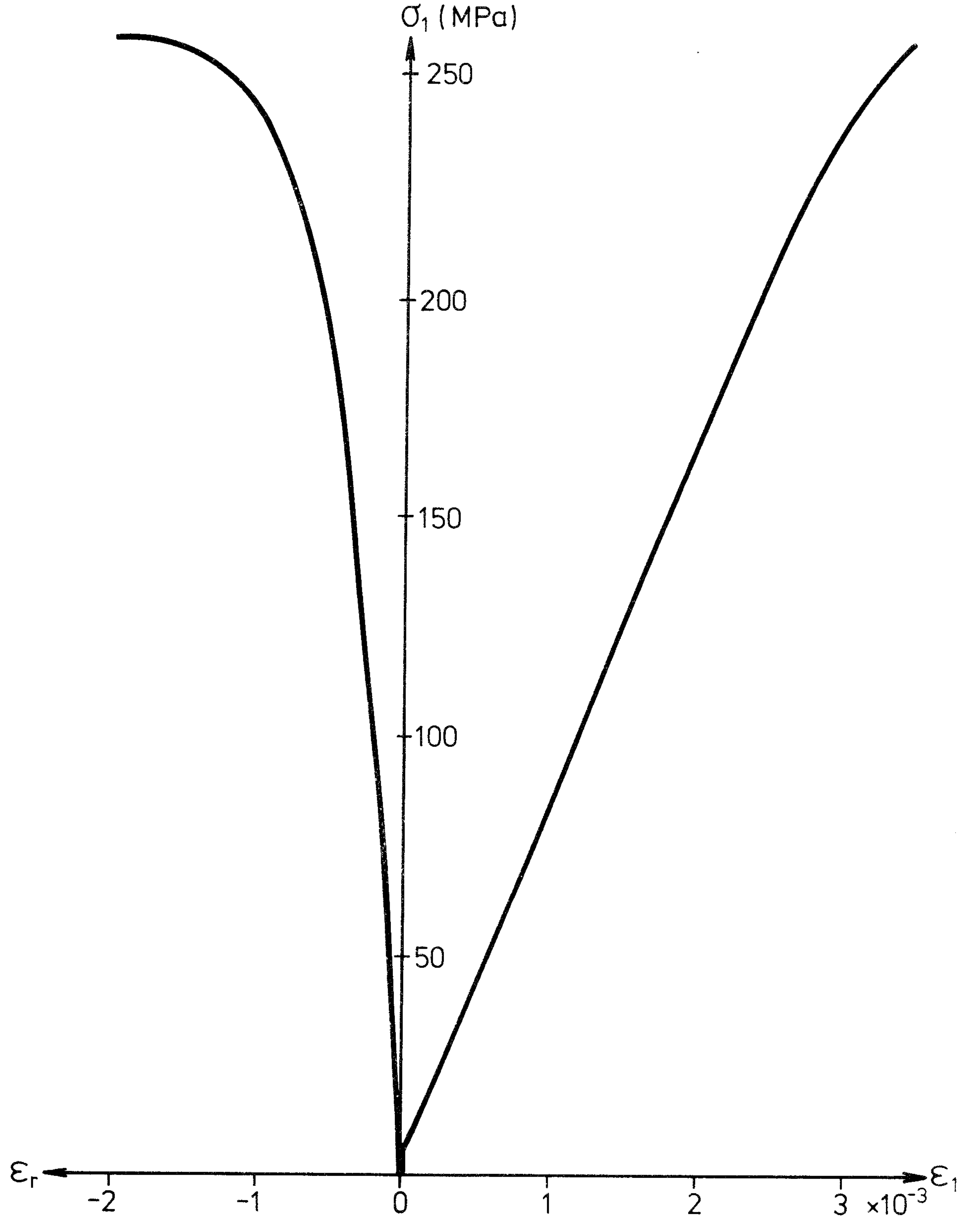


**Fig 2** TYPICAL STRESS-STRAIN PLOT FROM UNIAXIAL COMPRESSION TEST: FINNSJÖN GRANODIORITE.

PLATE 3

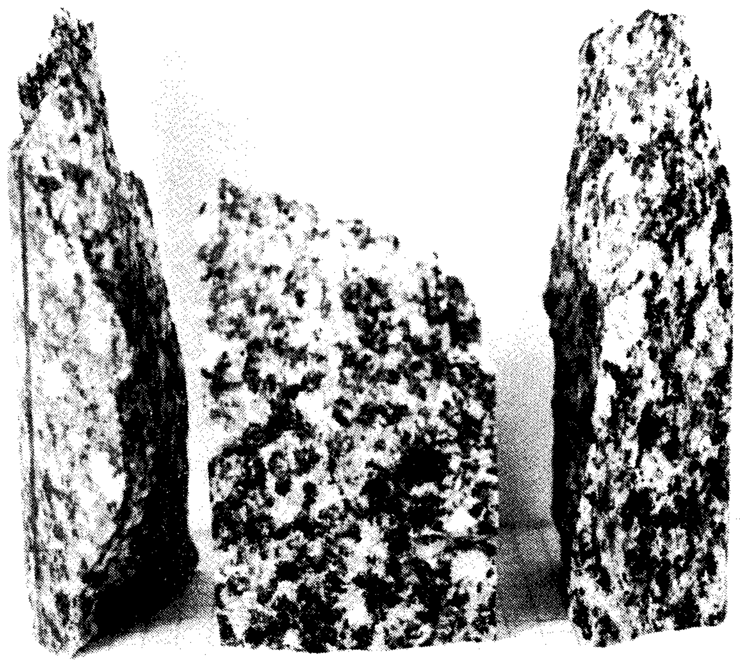

Appearance of failed specimen after uniaxial compression test: Finnsjön granodiorite. Note the vertical splitting which characterises the failure of this rock type.

PLATE 4

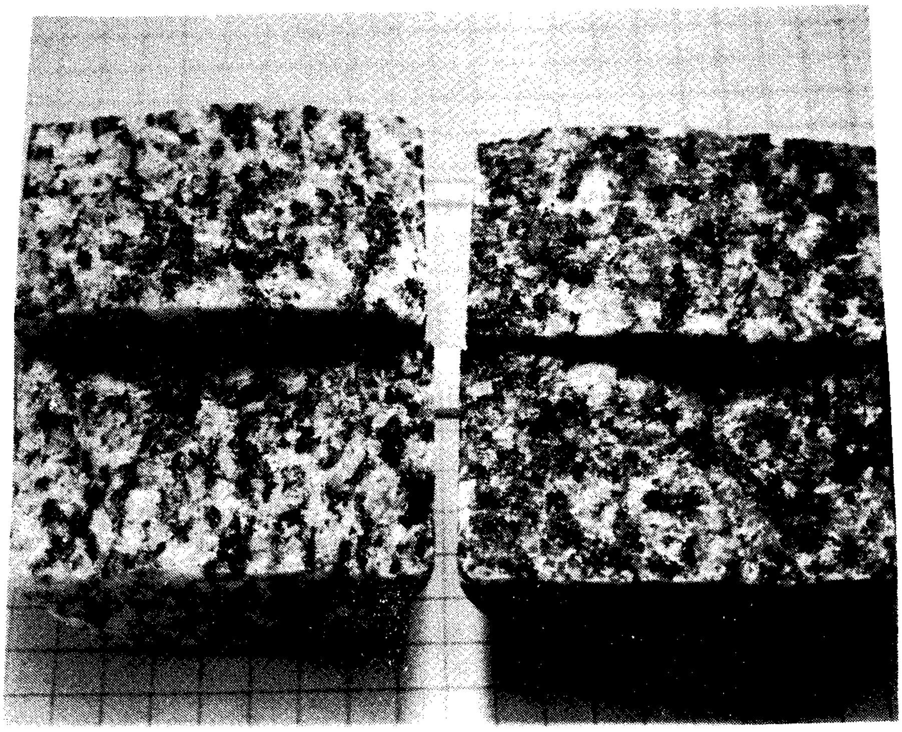

Appearance of failed specimens after Brazilian test: Finnsjön granodiorite.

Table IIIa

Comprehensive data: uniaxial compression tests

| Specimen number | Fracture stress $\sigma_c$ MPa | Young's Modulus E GPa | Poisson's ratio $\nu$ | Failure Description (see footnote) |
|---|---|---|---|---|
| FI 7.70 H1 | 233.0 | 87.6 | 0.21 | 1 |
| FI 8.90 H1 | 211.8 | 80.2 | 0.23 | 1,2 |
| FI 30.05 H1 | 254.2 | 82.8 | 0.18 | 1,2 |
| FI 31.20 H1 | 250.2 | 79.4 | 0.20 | 1,2 |
| FI 128.00 H1 | 238.3 | 74.5 | 0.17 | 1,2 |
| FI 130.10 H1 | 256.9 | 84.5 | 0.17 | 1 |
| FI 248.50 H1 | 247.6 | 83.9 | 0.22 | 1,2 |
| FI 249.50 H1 | 234.4 | 81.6 | 0.24 | 2 |
| FI 315.50 H1 | 251.6 | 82.8 | 0.18 | 1 |
| FI 317.50 H1 | 263.5 | 84.9 | 0.18 | 2 |
| FI 443.0 H1 | 223.8 | 85.3 | 0.18 | 1,2 |
| FI 444.0 H1 | 222.4 | 82.8 | 0.19 | 2 |

Table IIIb

Statistical summary, FINNSJÖN Hole 1

| FI - H1 | $\sigma_c$ (MPa) | E (GPa) | $\nu$ |
|---|---|---|---|
| mean | 240.6 | 82.5 | 0.20 |
| s.d. | 15.2 | 3.2 | 0.02 |

Note: 1. vertical splitting
2. failure on inclined plane (s)

Table IVa

Comprehensive data: "Brazilian" tests

| Specimen number | Failure Load P (kN) | Tensile fracture (MPa) |
|---|---|---|
| FI 7.6 H1 | 22.86 | 14.0 |
| FI 7.6 H1 | 23.04 | 14.1 |
| FI 29.8 H1 | 19.44 | 11.9 |
| FI 29.8 H1 | 22.14 | 13.6 |
| FI 128.0 H1 | 20.88 | 12.8 |
| FI 128.0 H1 | 16.20 | 9.9 |
| FI 248.4 H1 | 21.24 | 13.0 |
| FI 248.4 H1 | 21.60 | 13.3 |
| FI 317.4 | 26.10 | 16.0 |
| FI 317.4 | 27.00 | 16.6 |
| FI 442.9 H1 | 25.74 | 15.8 |
| FI 442.9 H1 | 17.64 | 10.8 |

Table IVb

Statistical summary, FINNSJÖN Hole 1.

| "Brazilian" fracture stress $\sigma_T$ | | |
|---|---|---|
| Rock Type | mean (MPa) | standard deviation |
| FINNSJÖN Bh 1 | 13.48 | 1.9 4 |

## 3.3 Blekinge Gneiss

For the single borehole (BL 1) from the Blekinge site, uniaxial compression test data is presented in Table Va, while Fig 3 shows a typical plot of axial stress against axial strain $\varepsilon_1$ and radial strain $\varepsilon_r$. A statistical summary of this data appears in Table Vb.

The complete data for the "Brazilian" tensile tests on the rock are given in Table VIa together with a statistical summary in Table VIb.

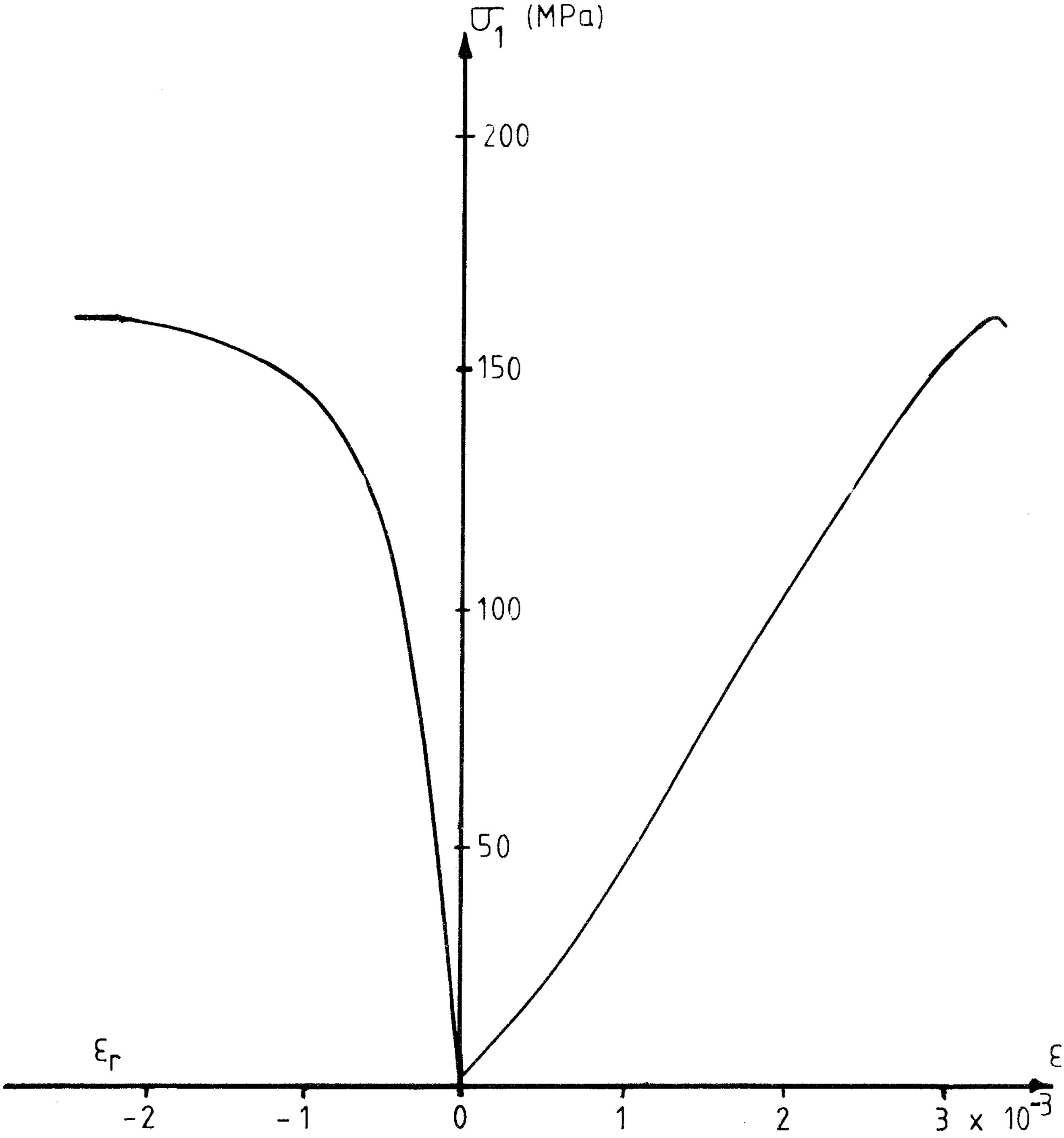


Fig 3 TYPICAL STRESS-STRAIN PLOT FROM UNIAXIAL COMPRESSION TEST: BLEKINGE GNEISS

Table Va
Comprehensive data: Uniaxial compression tests

| Specimen number | Fracture stress $\sigma_c$ MPa | Young´s Modulus E GPa | Poisson´s Ratio $\nu$ | Failure Description (see footnote) |
|---|---|---|---|---|
| BL 106.4 H1 | 133.0 | 51.2 | 0.19 | 1,2 |
| BL 107.0 H1 | 165.5 | 52.6 | 0.19 | 1,2 |
| BL 278.3 H1 | 153.9 | 56.8 | 0.20 | 2 |
| BL 279.1.H1 | 160.5 | 55.0 | 0.18 | 1,2 |
| BL 412.4 H1 | 192.0 | 67.4 | 0.26 | 1 |
| BL 414.2 H1 | 208.5 | 67.4 | 0.24 | 1,2 |

Table Vb
Statistical summary, BLEKINGE hole 1

| BL - H1 | $\sigma_c$ (MPa) | E (GPa) | $\nu$ |
|---|---|---|---|
| mean | 168.9 | 58.4 | 0.21 |
| s.d. | 24.8 | 6.6 | 0.03 |

Note: 1. vertical splitting
2. failure on inclined plane (s)

Table VIa

Comprehensive data:"Brazilian" tests

| Specimen number | Failure Load (kN) | Tensile fracture stress $\sigma_T$ (MPa) |
|---|---|---|
| BL 106.5 H1 | 12.2 | 7.0 |
| BL 106.9 H1 | 21.2 | 11.5 |
| BL 106.5 H1 | 14.0 | 7.9 |
| BL 107.1 H1 | 17.6 | 10.6 |
| BL 107.1 H1 | 17.6 | 10.7 |
| BL 278.4 H1 | 22.5 | 11.5 |
| BL 278.4 H1 | 21.2 | 11.1 |
| BL 279.1 H1 | 14.9 | 9.7 |
| BL 412.4 H1 | 18.0 | 13.1 |
| BL 412.4 H1 | 18.0 | 13.1 |
| BL 414.2 H1 | 17.1 | 11.7 |
| BL 414.2 H1 | 16.7 | 11.1 |

Table VIb

Statistical summary, BLEKINGE hole 1

| "Brazilian" fracture stress $\sigma_T$ | | |
|---|---|---|
| Rock Type | mean (MPa) | standard deviation |
| BLEKINGE Bh 1 | 10.75 | 1.75 |

## 4 DISCUSSION

For the four rock types investigated both reported here and in an earlier report (The mechanical properties of Stripa granite, K.B.S. 29:03), the mechanical properties (comprising Youngs Moduls, uniaxial compression failure stress, Brazilian tensile failure stress and Poissons ratio) are collected together in Table VII below. Considering this data on the basis of either the strength classification or the Modulus ratio classification of Deere and Miller [1] for example, it is clear that all the rocks in Table VII have a high quality designation. In particular, using the appropriate mechanical properties with reference to Tables VIII and IX, the quality classification given in Table X for each rock type is obtained.

Table VII
Mechanical properties of all the rock types investigated.

| Rock Type | Youngs Modulus, GPa | Compression Failure stress, MPa | Brazilian Failure stress, MPa | Poissons Ratio |
|---|---|---|---|---|
| KRÅKEMÅLA GRANITE H1 | 61 | 188 | 8.9 | 0.20 |
| KRÅKEMÅLA GRANITE H2 | 57 | 153 | 6.8 | 0.21 |
| FINNSJÖN GRANODIORITE | 83 | 241 | 13.5 | 0.20 |
| BLEKINGE GNEISS | 58 | 169 | 10.8 | 0.21 |
| STRIPA GRANITE | 69 | 207 | 15.0 | 0.21 |

Table VIII

Engineering classification of intact rock on basis of strength [1]

| Class | Description | Uniaxial compression Failure stress MPa |
|---|---|---|
| A | Very high | > 220 |
| B | High | 110 - 220 |
| C | Medium | 55 - 110 |
| D | Low | 28 - 55 |
| E | Very low | < 28 |

Table IX

Engineering classification of intact rock on basis of Modulus Ratio [1]

| Class | Description | Modulus ratio * |
|---|---|---|
| H | High | > 500 |
| M | Average | 200 - 500 |
| L | Low | < 200 |

* Modulus ratio = $E / \sigma_c$ [see 1]

Table X

Engineering classification of rocks tested.

| Rock type | Strength class. | Modulus ratio class. |
|---|---|---|
| KRÅKEMÅLA H1 | B | M |
| KRÅKEMÅLA H2 | B | M |
| FINNSJÖN | A | M |
| BLEKINGE | B | M |
| STRIPA | B | M |

## 5 REFERENCES

[1] DEERE and MILLER (1966), Engineering Classification and Index Properties of Intact Rock, Tech. Rept. N$^{o}$. AFWLTR-65-116, Air Force Weapons Lab, New Mexico.

FÖRTECKNING ÖVER KBS TEKNISKA RAPPORTER

01 Källstyrkor i utbränt bränsle och högaktivt avfall från en PWR beräknade med ORIGEN
Nils Kjellbert
AB Atomenergi 77-04-05

02 PM angående värmeledningstal hos jordmaterial
Sven Knutsson
Roland Pusch
Högskolan i Luleå 77-04-15

03 Deponering av högaktivt avfall i borrhål med buffertsubstans
Arvid Jacobsson
Roland Pusch
Högskolan i Luleå 77-05-27

04 Deponering av högaktivt avfall i tunnlar med buffertsubstans
Arvid Jacobsson
Roland Pusch
Högskolan i Luleå 77-06-01

05 Orienterande temperaturberäkningar för slutförvaring i berg av radioaktivt avfall, Rapport 1
Roland Blomqvist
AB Atomenergi 77-03-17

06 Groundwater movements around a repository, Phase 1, State of the art and detailed study plan
Ulf Lindblom
Hagconsult AB 77-02-28

07 Resteffekt studier för KBS
Del 1 Litteraturgenomgång
Del 2 Beräkningar
Kim Ekberg
Nils Kjellbert
Göran Olsson
AB Atomenergi 77-04-19

08 Utlakning av franskt, engelskt och kanadensiskt glas med högaktivt avfall
Göran Blomqvist
AB Atomenergi 77-05-20

09 Diffusion of soluble materials in a fluid filling a porous medium
Hans Häggblom
AB Atomenergi 77-03-24

10 Translation and development of the BNWL-Geosphere Model
Bertil Grundfelt
Kemakta Konsult AB 77-02-05

11 Utredning rörande titans lämplighet som korrosionshärdig kapsling för kärnbränsleavfall
Sture Henriksson
AB Atomenergi 77-04-18

12 Bedömning av egenskaper och funktion hos betong i samband med slutlig förvaring av kärnbränsleavfall i berg
Sven G Bergström
Göran Fagerlund
Lars Rombén
Cement- och Betonginstitutet 77-06-22

13 Urlakning av använt kärnbränsle (bestrålad uranoxid) vid direktdeponering
Ragnar Gelin
AB Atomenergi 77-06-08

14 Influence of cementation on the deformation properties of bentonite/quartz buffer substance
Roland Pusch
Högskolan i Luleå 77-06-20

15 Orienterande temperaturberäkningar för slutförvaring i berg av radioaktivt avfall
Rapport 2
Roland Blomquist
AB Atomenergi 77-05-17

16 Översikt av utländska riskanalyser samt planer och projekt rörande slutförvaring
Åke Hultgren
AB Atomenergi augusti 1977

17 The gravity field in Fennoscandia and postglacial crustal movements
Arne Bjerhammar
Stockholm augusti 1977

18 Rörelser och instabilitet i den svenska berggrunden
Nils-Axel Mörner
Stockholms Universitet augusti 1977

19 Studier av neotektonisk aktivitet i mellersta och norra Sverige, flygbildsgenomgång och geofysisk tolkning av recenta förkastningar
Robert Lagerbäck
Herbert Henkel
Sveriges Geologiska Undersökning september 1977

20 Tektonisk analys av södra Sverige, Vättern - Norra Skåne
Kennert Röshoff
Erik Lagerlund
Lunds Universitet och Högskolan Luleå september 1977

21 Earthquakes of Sweden 1891 - 1957, 1963 - 1972
Ota Kulhánek
Rutger Wahlström
Uppsala Universitet september 1977

22 The influence of rock movement on the stress/strain situation in tunnels or bore holes with radioactive consisters embedded in a bentonite/quartz buffer mass
Roland Pusch
Högskolan i Luleå 1977-08-22

23 Water uptake in a bentonite buffer mass
A model study
Roland Pusch
Högskolan i Luleå 1977-08-22

24 Beräkning av utlakning av vissa fissionsprodukter och aktinider från en cylinder av franskt glas
Göran Blomqvist
AB Atomenergi 1977-07-27

25 Blekinge kustgnejs, Geologi och hydrogeologi
Ingemar Larsson KTH
Tom Lundgren SGI
Ulf Wiklander SGU
Stockholm, augusti 1977

26 Bedömning av risken för fördröjt brott i titan
Kjell Pettersson
AB Atomenergi 1977-08-25

27 A short review of the formation, stability and cementing properties of natural zeolites
Arvid Jacobsson
Högskolan i Luleå 1977-10-03

28 Värmeledningsförsök på buffertsubstans av bentonit/pitesilt
Sven Knutsson
Högskolan i Luleå 1977-09-20

29 Deformationer i sprickigt berg
Ove Stephansson
Högskolan i Luleå 1977-09-28

30 Retardation of escaping nuclides from a final depository
Ivars Neretnieks
Kungliga Tekniska Högskolan Stockholm 1977-09-14

31 Bedömning av korrosionsbeständigheten hos material avsedda för kapsling av kärnbränsleavfall. Lägesrapport 1977-09-27 samt kompletterande yttranden.
Korrosionsinstitutet och dess referensgrupp

32 Long term mineralogical properties of bentonite/quartz buffer substance
Preliminär rapport november 1977
Slutrapport februari 1978
Roland Pusch
Arvid Jacobsson
Högskolan i Luleå

33 Required physical and mechanical properties of buffer masses
Roland Pusch
Högskolan Luleå 1977-10-19

34 Tillverkning av bly-titan kapsel
Folke Sandelin AB
VBB
ASEA-Kabel
Institutet för metallforskning
Stockholm november 1977

35 Project for the handling and storage of vitrified high-level waste
Saint Gobain Techniques Nouvelles October, 1977

36 Sammansättning av grundvatten på större djup i granitisk berggrund
Jan Rennerfelt
Orrje & Co, Stockholm 1977-11-07

37 Hantering av buffertmaterial av bentonit och kvarts
Hans Fagerström, VBB
Björn Lundahl, Stabilator
Stockholm oktober 1977

38 Utformning av bergrumsanläggningar
Arne Finné, KBS
Alf Engelbrektson, VBB
Stockholm december 1977

39 Konstruktionsstudier, direktdeponering
ASEA-ATOM
VBB
Västerås

40 Ekologisk transport och stråldoser från grundvattenburna radioaktiva ämnen
Ronny Bergman
Ulla Bergström
Sverker Evans
AB Atomenergi

41 Säkerhet och strålskydd inom kärnkraftområdet.
Lagar, normer och bedömningsgrunder
Christina Gyllander
Siegfried F Johnson
Stig Rolandson
AB Atomenergi och ASEA-ATOM

42 Säkerhet vid hantering, lagring och transport av använt kärnbränsle och förglasat högaktivt avfall
Ann Margret Ericsson
Kemakta november 1977

43 Transport av radioaktiva ämnen med grundvatten från ett bergförvar
Bertil Grundfelt
Kemakta november 1977

44 Beständighet hos borsilikatglas
Tibor Lakatos
Glasteknisk Utveckling AB

45 Beräkning av temperaturer i ett envånings slutförvar i berg för förglasat radioaktivt avfall Rapport 3
Roland Blomquist
AB Atomenergi 1977-10-19

46 Temperaturberäkningar för använt bränsle
Taivo Tarandi
VBB

47 Teoretiska studier av grundvattenrörelser
Preliminär rapport oktober 1977
Slutrapport februari 1978
Lars Y Nilsson
John Stokes
Roger Thunvik
Inst för kulturteknik KTH

48 The mechanical properties of the rocks in Stripa, Kråkemåla, Finnsjön and Blekinge
Graham Swan
Högskolan i Luleå 1977-09-14

49 Bergspänningsmätningar i Stripa gruva
Hans Carlsson
Högskolan i Luleå 1977-08-29

50 Lakningsförsök med högaktivt franskt glas i Studsvik
Göran Blomqvist
AB Atomenergi november 1977

51 Seismotechtonic risk modelling for nuclear waste disposal in the Swedish bedrock
F Ringdal
H Gjöystdal
E S Hysebye
Royal Norwegian Council for scientific and industrial research

52 Calculations of nuclide migration in rock and porous media, penetrated by water
H Häggblom
AB Atomenergi 1977-09-14

53 Mätning av diffusionshastighet för silver i lera-sand-blandning
Bert Allard
Heino Kipatsi
Chalmers tekniska högskola 1977-10-15

54 Groundwater movements around a repository

54:01 Geological and geotechnical conditions
Håkan Stille
Anthony Burgess
Ulf E Lindblom
Hagconsult AB september 1977

54:02 Thermal analyses
Part 1 Conduction heat transfer
Part 2 Advective heat transfer
Joe L Ratigan
Hagconsult AB september 1977

54:03 Regional groundwater flow analyses
Part 1 Initial conditions
Part 2 Long term residual conditions
Anthony Burgess
Hagconsult AB oktober 1977

54:04 Rock mechanics analyses
Joe L Ratigan
Hagconsult AB september 1977

54:05 Repository domain groundwater flow analyses
Part 1 Permeability perturbations
Part 2 Inflow to repository
Part 3 Thermally induced flow
Joe L Ratigan
Anthony S Burgess
Edward L Skiba
Robin Charlwood

54:06 Final report
Ulf Lindblom et al
Hagconsult AB oktober 1977

55 Sorption av långlivade radionuklider i lera och berg
Del 1 Bestämning av fördelningskoefficienter
Del 2 Litteraturgenomgång
Bert Allard
Heino Kipatsi
Jan Rydberg
Chalmers tekniska högskola 1977-10-10

56 Radiolys av utfyllnadsmaterial
Bert Allard
Heino Kipatsi
Jan Rydberg
Chalmers tkniska högskola 1977-10-15

57 Stråldoser vid haveri under sjötransport av kärnbränsle
Anders Appelgren
Ulla Bergström
Lennart Devell
AB Atomenergi

58 Strålrisker och högsta tillåtliga stråldoser för människan
Gunnar Walinder
FOA 4 november 1977